Fusion of ^{48}Ca + ^{90,96}Zr above and below the Coulomb barrier

A. M. Stefanini,[1] F. Scarlassara,[2] S. Beghini,[2] G. Montagnoli,[2] R. Silvestri,[2] M. Trotta,[3] B. R. Behera,[1] L. Corradi,[1] E. Fioretto,[1] A. Gadea,[1] Y. W. Wu,[1] S. Szilner,[4] H. Q. Zhang,[5] Z. H. Liu,[5] M. Ruan,[5] F. Yang,[5] and N. Rowley[6]

[1]*INFN, Laboratori Nazionali di Legnaro, I-35020 Legnaro (Padova), Italy*

[2]*INFN and Dipartimento di Fisica, Universitá di Padova, I-35131 Padova, Italy*

[3]*INFN, Sezione di Napoli, I-80126 Napoli, Italy*

[4]*Ruder Bosković Institute, HR-10002 Zagreb, Croatia*

[5]*China Institute of Atomic Energy, 102413 Beijing, China*

[6]*IReS, UMR7500, IN2P3-CNRS/Université Louis Pasteur, Boîte Postale28, F-67037 Strasbourg Cedex 2, France*

(Received 20 December 2005; published 15 March 2006)

Fusion-evaporation cross sections were measured in the two systems ^{48}Ca + ^{90,96}Zr in an energy range from well below to well above the Coulomb barrier. The sub-barrier fusion of ^{48}Ca + ^{90}Zr is reproduced by coupled-channels calculations including the lowest quadrupole and octupole vibrations of ^{90}Zr, and using a Woods-Saxon potential with a standard diffuseness parameter $a = 0.68$ fm. However, the fusion cross sections are overestimated above the barrier. The low-energy slope of the excitation function for ^{48}Ca + ^{96}Zr is steeper. This implies a larger diffuseness parameter $a = 0.85$ fm. Fusion cross sections are well fit in the whole energy range, and the effect of the strong octupole vibration in ^{96}Zr is predominant. The extracted fusion barrier distributions are reasonably well reproduced by calculations for both systems. A comparison with previous data for ^{40}Ca + ^{90,96}Zr is made in an attempt to clarify the role of transfer couplings in sub-barrier fusion.

DOI: 10.1103/PhysRevC.73.034606 PACS number(s): 25.70.Jj, 24.10.Eq

I. INTRODUCTION

Heavy-ion fusion dynamics at energies near and below the Coulomb barrier has been the subject of many experimental and theoretical studies for more than 20 years [1,2], using stable beams and, more recently, radioactive beams as well. Sub-barrier fusion cross sections are generally dominated by strong couplings to nuclear shape vibrations, deformations, and, possibly, nucleon-transfer degrees of freedom. The method of extracting fusion barrier distributions from the second energy derivative of the fusion excitation function [3] has been a major breakthrough in understanding the kind of couplings involved in the various cases, thus clarifying the intimate links between nuclear structure and reaction dynamics. However, treating nucleon-transfer couplings correctly in theoretical models to predict their effects on near- and sub-barrier fusion cross sections remains a challenge.

Previous experiments on the sub-barrier fusion of ^{40}Ca + ^{90,96}Zr [4] showed a striking difference between the two excitation functions and the extracted barrier distributions. This was attributed to couplings to neutron pickup transfer channels with positive Q values, which only exist for ^{40}Ca + ^{96}Zr. However, a more recent analysis [5] showed that both sub-barrier fusion enhancements and the shape of the barrier distributions can be reproduced within a semiclassical model [6], which suggests that most of the isotopic difference should be attributed to the strong octupole vibration of ^{96}Zr. Moreover, the "quantum molecular dynamics model" of Wang *et al.* [7] predicts, for both ^{48}Ca + ^{90}Zr and, ^{48}Ca + ^{96}Zr, sub-barrier fusion cross sections larger than for ^{40}Ca + ^{96}Zr, as a consequence of the neutron richness of the systems. The simplified model of Zagrebaev [8], which takes into account the effect of neutron transfer in an approximate way, reproduces the ^{40}Ca + ^{90,96}Zr excitation functions correctly.

The first motivation of the present work, therefore, was to try to clarify the situation by means of further experimental information for fusion involving ^{90}Zr and ^{96}Zr, but using a ^{48}Ca projectile, which is magic and more rigid than ^{40}Ca (where a strong octupole vibration exists) and which does not give rise to any neutron transfers with positive ground-state Q values with either zirconium isotope.

It has also been recently recognized [9] that several fusion excitation functions in the above-barrier energy range can be best fitted with a diffuseness parameter a of the usual Woods-Saxon parametrization of the nuclear potential in the range $a = 0.75$ to 1.5 fm, that is, much larger than the value $a \approx 0.65$ fm generally deduced from fits to elastic scattering data. The fusion cross sections are systematically overpredicted when using this lower value. The underlying reason or reasons are not yet clear. Various suggestions have been made, among which we cite the inability of a static potential to describe the reaction dynamics over a broad energy range, and the competition with dissipative reactions other than fusion (such as deep inelastic collisions [9,10]), which might reduce the fusion cross section and lead to the (artificial) need of a large "effective" diffuseness to simulate this.

However, the diffuseness parameter a determines the slope of the potential in its tail, that is, in the region of the Coulomb barrier where fusion takes place. Hence a is directly connected to the width of the barrier (see [10] and references therein), and it determines the rate of change of the fusion cross section below the "lowest" barrier in the picture of a barrier distribution that arises as a consequence of channel couplings. As a matter of fact, one can show [11] that the width of the barrier is roughly proportional to $a^{-1/2}$. It is also worth noting that the diffuseness parameter can, of course, influence the coupling strengths. To first order, they are proportional to the deformation length and to $dV_{\rm Nucl}/dr$. However, at the

Coulomb barrier $dV_{\rm Nucl}/dr + dV_{\rm Coulomb}/dr = 0$, so that as long as the other potential parameters are changed to keep the barrier height fixed, changing a has, in fact, little effect on the couplings strengths near the barrier.

When lowering the energy in the sub-barrier region, fusion excitation functions usually show an exponential decrease [12]. However, recent studies [13,14] of deep sub-barrier fusion cross sections have revealed somewhat unexpected effects, beyond the known approximations of the Wong formula. Usually, the logarithmic derivative $d\ln(E\sigma)/d$E shows a steep rise in the barrier region with decreasing energy and then levels off around the energy where the barrier distribution vanishes. For a number of systems, however, it has been found that the derivative continues increasing at even lower energies, implying so-called hindrance effects, whose origin is a matter of current discussion [15–20].

One notices that a large diffuseness parameter a, as invoked to fit the data of several systems above the barrier, would produce a steep decrease of the fusion cross section below the lowest barrier, provided that the "lowest barrier" has been clearly identified with the help of the barrier distribution representation (but identification of the "lowest barrier" is not always obvious). The second motivation of the present study has been, therefore, to try to reproduce the excitation functions of ^{48}Ca + ^{90,96}Zr over the whole measured energy range within a Coupled Channels (CC) model employing a nuclear potential of Woods-Saxon (WS)shape. Here the specific aim was to deduce information on the diffuseness a needed for the two systems. Fitting the sub-barrier fusion cross sections with the same parameter a used in the high-energy region would give us confidence that modeling the fusion dynamics on the basis of a static WS nuclear potential is correct.

A preliminary and brief account of the data reported in this paper was presented in Ref. [21]. Here the analysis has been extended and completed. The description of the experimental setup and procedures in Sec. II is followed by a discussion of the low-energy trends of the two excitation functions in Sec. III. Then the results of coupled-channels calculations are presented in Sec. IV, fusion barrier distributions are discussed in Sec. V, and a brief comparison is made with the aforementioned cases ^{40}Ca + ^{90,96}Zr in Sec. VI. Section VII is a summary of the main results of the present work.

II. EXPERIMENTAL

The experiments reported here used ^{48}Ca beams produced by a sputter ion source. A metallic calcium sample, enriched to $\simeq$65% in mass 48, was sprayed with ammonia and the resulting CaH^- ions were injected into the XTU Tandem accelerator of the Laboratori Nazionali di Legnaro of INFN. Beam intensities on target were $\simeq$3–7 pnA in the energy range 133–174 MeV (from $\approx$7%–8% below to $\approx$17%–18% above the Coulomb barriers).

The 90° analyzing magnet of the XTU Tandem defined the beam energy to better than 1/800 [22]. Hysteresis effects were minimized by changing the energy only downward in the measurements of the excitation functions, and by using the same ion charge state (10^+) in the relevant range from 160 to 133 MeV. A fluorescent quartz was employed to focus the beams to the same position on the targets for each run.

The targets were evaporations of metallic ^{90}Zr (50 μg/cm^2) and of $^{96}ZrO_2$ (50 μg/cm^2) on carbon backings (15 μg/cm^2) facing the beam. The isotopic enrichments were 99.4% and 95.6%, respectively. The targets were placed in a Ø = 100 cm scattering chamber. The beam energy losses in the carbon backings ($\simeq$180 keV) and in the targets were taken into account in the data analysis.

Four silicon detectors monitored the beam by measuring the Rutherford scattering from the target. They were placed above and below and to the left and right of the beam at the same scattering angle $\theta_{\rm lab} = 16°$. The observed variations of the relative yields in these monitors, owing to small changes of beam focusing and position in the various runs, permitted appropriate corrections to the fusion-evaporation residue cross sections.

The evaporation residues (ER) were separated from the background of beam and beam-like particles at 0° and nearby angles by means of an electrostatic deflector [23]. The beam ions were stopped at the exit of the deflector, whereas ER were detected by an energy time-of-flight telescope consisting of a microchannel plate detector and a 300 mm^2 silicon surface-barrier detector. The beam rejection factor of the setup is $\simeq 10^8$, with an effective solid angle $\simeq$25 μsr. ER angular distributions were measured for the two systems at $E_{\rm lab} = 166$ and 150 MeV (and also at 142 MeV for ^{48}Ca + ^{96}Zr) in the range $-4°$–$+5°$, with 1° steps, in addition to the 0° excitation functions. No significant variation with energy of the width of the angular distribution was observed. Figure 1 shows two typical time

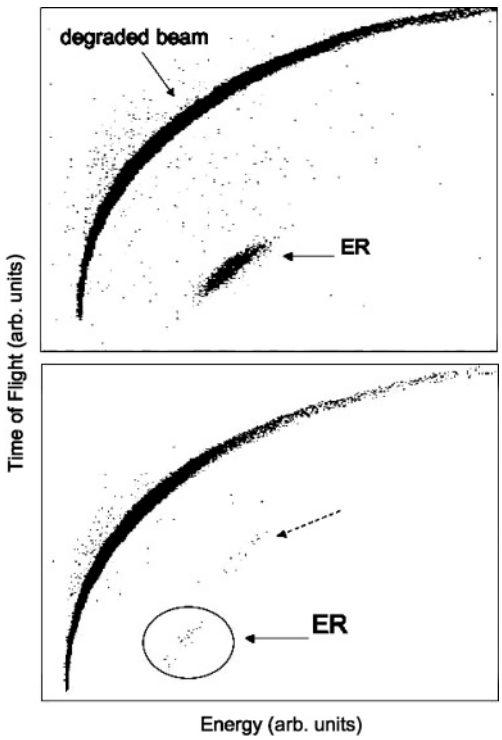

FIG. 1. Time of flight vs energy spectra measured for 144.2-MeV ^{48}Ca + ^{96}Zr (top) and 139.8-MeV ^{48}Ca + ^{90}Zr (bottom); see text.

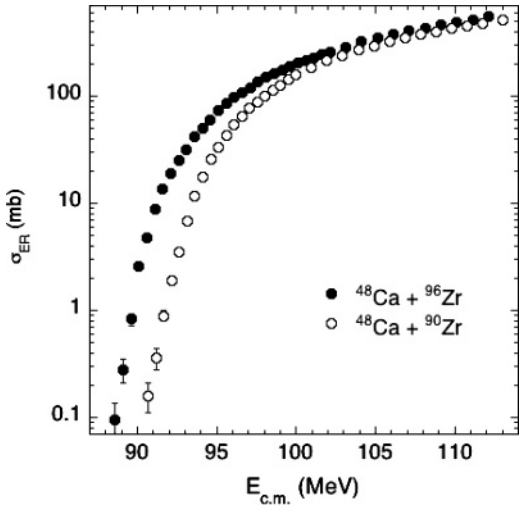

FIG. 2. Fusion-evaporation cross sections for ^{48}Ca + ^{90,96}Zr.

of flight versus energy spectra measured at 0°. In the upper panel one notices the group of ER clearly separated from the energy-degraded beamlike particles. The ER cross section at that energy (144.2 MeV) is 97 mb, and ≈5000 ER were registered in a run of around 30 min duration. In the lower panel, the ER are highlighted by the circle. Here σ_{ER} is 360 μb, and only 20 ER were detected in 2 h. The spectrum is, in any case, very clean. The dashed line indicates a group of events probably produced by fusion of the ^{48}Ca beam with the carbon backing of the target.

Since fusion-fission is negligible for the present systems (see also Ref. [4]), total fusion cross sections were derived from the normalized 0° ER yields, from the angular distributions, and from the transmission of the electrostatic deflector $T = 0.70 \pm 0.05$ measured for the similar cases ^{40}Ca + ^{90,96}Zr [4]. This value was independently checked by Monte Carlo simulations for the present systems. Absolute cross sections have a systematic uncertainty ±14% (see Refs. [22,24]), whereas relative errors are mainly determined by statistics. Figure 2 shows the measured fusion cross sections for ^{48}Ca + ^{90,96}Zr. Only statistical uncertainties are reported. The cross sections are listed in Tables I and II.

III. LOW-ENERGY TRENDS

The low-energy behavior of the excitation functions is best displayed and compared by plotting the logarithmic derivative $d\ln(E\sigma)/dE$ of the cross section versus energy. This is shown in Fig. 3 for ^{48}Ca + ^{90,96}Zr. Each plotted value of the derivative has been simply obtained from two adjacent points of the excitation function, and the quoted errors follow from the statistical (relative) uncertainty of the two points considered.

The present data do not extend into the deep sub-barrier energy range; nevertheless, considering the low-energy excitation functions allows interesting observations at the qualitative level. Already from Fig. 2, one notices that the excitation function for ^{48}Ca + ^{96}Zr is visibly steeper at the lowest measured energies. This is amplified in the representation of the logarithmic derivatives of Fig. 3. The data for ^{48}Ca + ^{96}Zr probably show the expected low-energy plateau below $E \simeq 90$ MeV, at the level of $\simeq$2.2 MeV^{-1} for the logarithmic slope (with the three lowest points being the same within the experimental errors). As for ^{48}Ca + ^{90}Zr, it is less clear from the data whether the curve levels off at the lowest energies, where the logarithmic derivative is $\simeq$1.7 MeV^{-1}, that is, ≈25% smaller than the saturation value for ^{48}Ca + ^{96}Zr. The difference in the low-energy trends between the two systems is not obvious a priori. One might point to the possible influence of neutron-transfer channels. However, apart from couplings to inelastic excitations (see next section), neutron-transfer

TABLE I. Fusion cross sections for ^{48}Ca + ^{90}Zr. Quoted errors are statistical uncertainties only.

$E_{c.m.}$ (MeV)	σ_{ER} (mb)	$E_{c.m.}$ (MeV)	σ_{ER} (mb)
90.7	0.16 ± 0.05	99.0	127.2 ± 1.8
91.2	0.36 ± 0.08	99.5	141.9 ± 1.8
91.7	0.89 ± 0.10	100.0	157.7 ± 1.6
92.2	1.89 ± 0.17	101.0	186.3 ± 1.9
92.7	3.50 ± 0.27	102.0	214.0 ± 2.3
93.1	6.80 ± 0.56	102.9	241.9 ± 2.6
93.6	11.8 ± 0.70	103.9	269.1 ± 2.2
94.1	17.7 ± 1.1	104.9	295.7 ± 3.1
94.6	25.6 ± 1.5	105.9	322.8 ± 3.5
95.1	33.7 ± 0.8	106.9	347.9 ± 3.4
95.6	43.3 ± 0.9	107.8	374.5 ± 4.0
96.1	54.0 ± 1.0	108.8	402.0 ± 4.0
96.6	65.3 ± 1.3	109.8	426.5 ± 4.1
97.1	77.1 ± 1.5	110.8	455.0 ± 5.0
97.6	89.0 ± 1.7	111.8	479.8 ± 5.2
98.0	100.9 ± 1.8	113.1	516.9 ± 5.8
98.5	113.8 ± 1.7		

TABLE II. Fusion cross sections for ^{48}Ca + ^{96}Zr. Quoted errors are statistical uncertainties only.

$E_{c.m.}$ (MeV)	σ_{ER} (mb)	$E_{c.m.}$ (MeV)	σ_{ER} (mb)
88.6	0.095 ± 0.040	98.1	149.4 ± 2.8
89.1	0.28 ± 0.07	98.6	161.5 ± 2.9
89.6	0.83 ± 0.11	99.1	174.9 ± 2.9
90.1	2.59 ± 0.25	99.6	189.1 ± 3.2
90.6	4.73 ± 0.31	100.1	203.9 ± 3.4
91.1	8.73 ± 0.40	100.6	215.7 ± 3.5
91.6	13.5 ± 0.65	101.1	230.0 ± 3.3
92.1	18.9 ± 0.6	101.6	244.9 ± 4.4
92.6	25.2 ± 0.9	102.1	257.4 ± 2.7
93.1	31.5 ± 1.0	103.1	289.9 ± 3.2
93.6	41.8 ± 1.2	104.1	325.1 ± 3.4
94.1	49.8 ± 1.5	105.1	349.4 ± 4.4
94.6	60.5 ± 1.7	106.1	381.0 ± 4.1
95.1	73.0 ± 2.4	107.1	407.4 ± 4.5
95.6	85.7 ± 2.7	108.1	433.5 ± 4.6
96.1	96.6 ± 3.1	109.1	464.9 ± 4.8
96.6	108.4 ± 3.0	110.1	494.0 ± 5.1
97.1	121.0 ± 2.7	111.1	522.0 ± 5.2
97.6	134.9 ± 2.8	112.1	552.0 ± 5.7

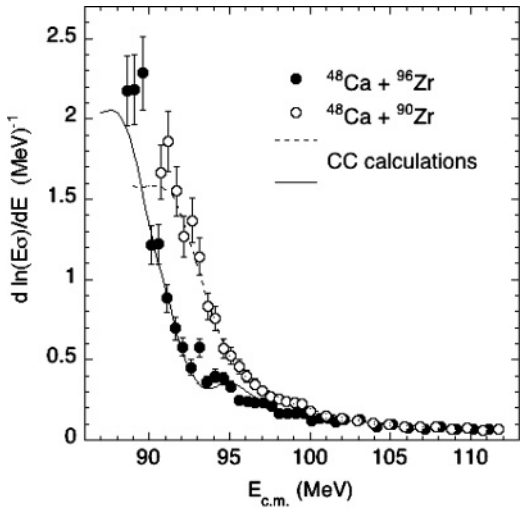

FIG. 3. Logarithmic derivatives of the excitation functions.

channels are not expected to play a role in the present cases, since no transfer channel with positive Q value exists in either system. Only proton pickups can have positive Q values for ^{48}Ca + ^{90}Zr. All this calls for further measurements at deeper sub-barrier energies, which, unfortunately, are not possible with our present setup.

IV. COUPLED-CHANNELS CALCULATIONS

Coupled-channels calculations have been performed with the code CCFULL, where the WS parametrization of the nuclear potential is adopted. A detailed description of the program, its physical background, and some inherent approximations can be found in Ref. [25]. In particular, coupling strengths are taken into account to all orders, and higher phonon states may be included by treating vibrational couplings in the harmonic limit. A point should be made here: using the harmonic limit may generate some problems in associating the results of calculations to the real structure of the colliding nuclei (usually far from being harmonic oscillators), the more so when two- and possibly three-phonon excitations appear to influence the fusion cross sections considerably [26]. This is actually the case for the present systems involving zirconium isotopes, which are heavy and relatively soft with respect to quadrupole and octupole vibrations.

After this preamble, we show in Table III the relevant information on the low-lying excitations of ^{48}Ca, ^{90}Zr, and ^{96}Zr. The quadrupole vibrations of ^{90,96}Zr are both weak and lie at comparable energies. The 5^- state of ^{90}Zr was included in the CC calculations by renormalizing the nuclear coupling strength of the 2^+ state [27]. The octupole vibration in ^{96}Zr is significantly stronger and lower in energy than in ^{90}Zr. The magic nucleus ^{48}Ca is very rigid; in the calculations, only the relatively strong 3^- state was included in the coupling scheme. The effect of its high excitation energy is nearly adiabatic, that is, a renormalization [28] of the nuclear potential occurs, producing a lower Coulomb barrier, with little influence on the shape of the fusion barrier distribution.

TABLE III. Excitation energies E_x, spin and parities λ^π, and deformation parameters β_λ [29,30] (see text).

Nucleus	E_x(MeV)	λ^π	β_λ
^{48}Ca	3.832	2^+	0.11
	4.507	3^-	0.23
^{90}Zr	2.186	2^+	0.09
	2.748	3^-	0.22
	(2.319	5^-	0.12)
^{96}Zr	1.751	2^+	0.08
	1.897	3^-	0.27

For both systems, obtaining reasonable fits to the excitation functions requires target vibrations of quadrupole and octupole character to be included up to the two-phonon level for each mode, as well as mutual excitations of the type $2^+ \otimes 3^-$, $(2^+)^2 \otimes 3^-$, $2^+ \otimes (3^-)^2$, and $(2^+)^2 \otimes (3^-)^2$. Mutual excitations between projectile and target states are also taken into account. For ^{48}Ca + ^{96}Zr only, the three-phonon state $(3^{-})^3$ has a non-negligible effect at low energies.

The parameters of the Akyüz-Winther (AW) potentials [31] are reported in Table IV together with those of the modified potentials used in the present CC calculations that include the low-lying vibrations of projectile and target. The analysis with CCFULL was performed along the following lines. First, a good fit to the slope in the sub-barrier energy region was searched for, determining (qualitatively) the value of the diffuseness parameter a. After this, the height of the barrier was slightly varied with respect to the AW value (r_o was varied and V_o consequently), to achieve a good fit near and below the Coulomb barrier. It turns out that the adiabatic effect of the high-lying 3^- state of ^{48}Ca brings the "effective " barrier very near to the original AW value in both systems.

We consider first ^{48}Ca + ^{96}Zr. The calculation reproduces the data below and above the barrier (see Fig. 4, upper panel), only by adopting a diffuseness parameter $a = 0.85$ fm, larger than the AW value. This is in agreement with the systematics of Newton *et al*. [9]. The logarithmic derivative of the calculated excitation function, shown in Fig. 3, closely resembles the data trend.

TABLE IV. Parameters of the Akyüz-Winther potential [31] (first line for each system) and those employed in our CC calculations (second line, see text) together with barrier heights, radii, and curvatures resulting from the previous potentials.

System	V_o (MeV)	r_o (fm)	a (fm)
^{48}Ca + ^{90}Zr	73.7	1.18	0.68
	113.9	1.12	0.68
^{48}Ca + ^{96}Zr	73.3	1.18	0.68
	127.8	1.05	0.85
	V_b (MeV)	R_b (fm)	$\hbar\omega$ (MeV)
^{48}Ca + ^{90}Zr	96.9	11.08	3.58
	98.3	10.95	3.76
^{48}Ca + ^{96}Zr	95.9	11.21	3.51
	97.5	10.82	3.25

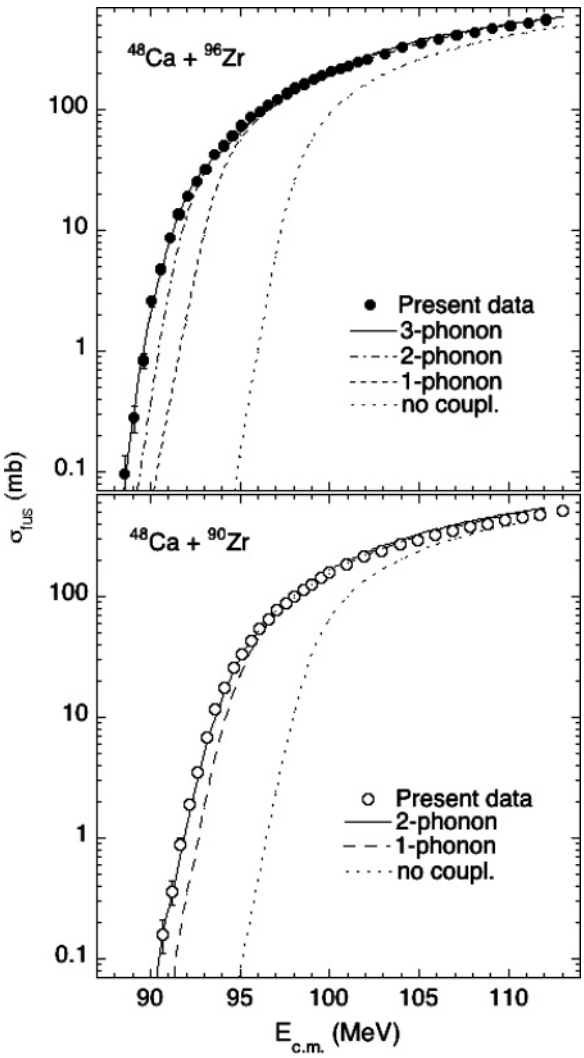

FIG. 4. Measured fusion cross sections of ^{48}Ca + ^{90,96}Zr, in comparison with CC calculations.

In the case of ^{48}Ca + ^{90}Zr (lower panel of Fig. 4) the standard diffuseness $a = 0.68$ fm gives a good fit to the data at near- and sub-barrier energies, by including the aforementioned vibrational couplings (solid line). The logarithmic derivatives of data and calculation for ^{48}Ca + ^{90}Zr are shown in Fig. 3, where the agreement can be better appreciated. However, the cross sections are overpredicted above the barrier (see Fig. 4) by 12%–13%, which is still (marginally) within the overall accuracy of the absolute cross section scale. Correcting for this disagreement would require a larger diffuseness [9], but the good fit at low energies would be lost.

The situation is better represented in Fig. 5, where the solid line is the same calculation reported in Fig. 4, and the dashed line is the calculation with $a = 0.90$ fm, that is, the value used in Ref. [4] for ^{40}Ca + ^{90}Zr. The value of r_o was adjusted to give the same barrier $V_b = 98.3$ MeV as for the solid line. The dashed line clearly fails to reproduce the sub-barrier energy dependence of the excitation function. Conversely, keeping $a = 0.68$ fm and varying the Coulomb barrier, through r_o and V_o, to get a good fit above the barrier (dashed-dotted

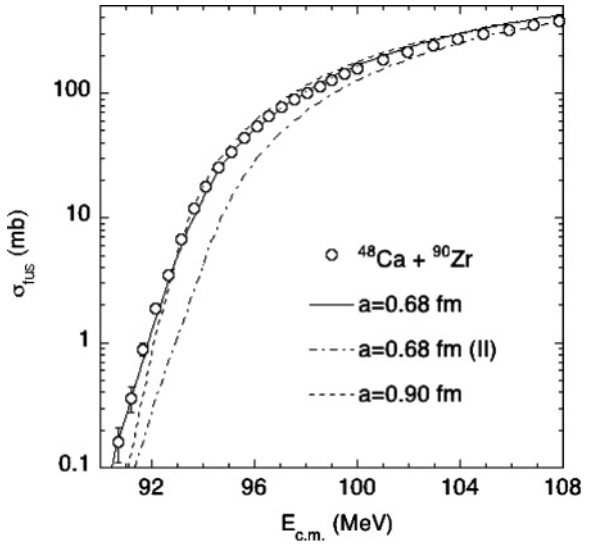

FIG. 5. Fusion excitation function of ^{48}Ca + ^{90}Zr in a slightly expanded view with respect to Fig. 4. The solid line is the same calculation reported in Fig. 4; the dashed line uses a larger diffuseness, but the barrier is not varied. The dashed-dotted line keeps $a = 0.68$ fm and the barrier is increased to best fit the high-energy data points (see text).

line) leads to a large underprediction of the sub-barrier cross sections. This cannot be compensated for by introducing additional channels in the coupling scheme, since three-phonon excitations have very little effect, and the Q values for all transfer channels are large and negative in this system.

As a partial conclusion, we may say that both ^{48}Ca + ^{90}Zr and ^{48}Ca + ^{96}Zr require a diffuseness parameter of the WS potential significantly larger than the AW value to achieve a good fit to the fusion cross sections above the barrier. The physical reasons behind this observation should certainly be investigated [9] further. However, there is a difference between the two systems below the barrier. For ^{48}Ca + ^{96}Zr, the "large" $a = 0.85$ fm allows one to reproduce correctly the sub-barrier cross sections, but this is not the case with ^{48}Ca + ^{90}Zr, where a standard value $a \simeq 0.68$ fm is required. Moreover, the AW potential used in the CC calculations for ^{48}Ca + ^{96}Zr has a smaller radius parameter r_o than for ^{48}Ca + ^{90}Zr (1.05 versus 1.12 fm). This is not the result of a χ^2 fit, but the trend is the same as noted by Newton *et al.* [9] for ^{40}Ca + ^{90,96}Zr. Presently, we have no physical explanation for these isotopic effects.

V. BARRIER DISTRIBUTIONS

The fusion barrier distributions for ^{48}Ca + ^{90,96}Zr have been obtained [3] by double differentiation of $E\sigma_{fus}$ with respect to the energy, using the three-point difference formula [4] with an energy step $\Delta E = 2$ MeV. They are shown in Fig. 6, normalized to unity. Concerning ^{48}Ca + ^{90}Zr, the shape of the distribution is clear, with two main peaks around 94 and 98 MeV. It is very similar to what is obtained for ^{40}Ca + ^{90}Zr [4]. The calculation marked "1-phonon " (that is, one quadrupole phonon and one octupole phonon; dashed line)

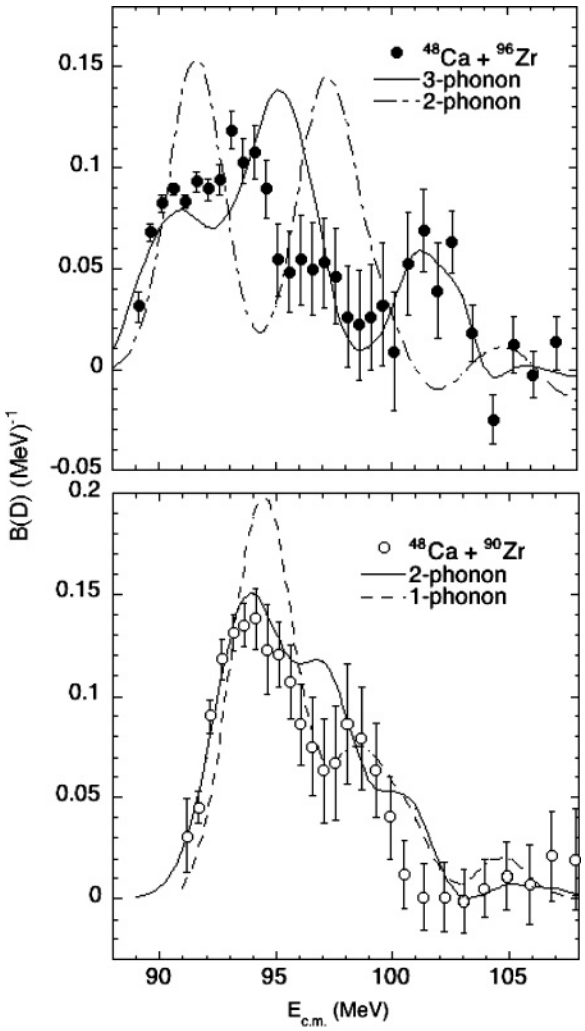

FIG. 6. Fusion barrier distributions of ^{48}Ca + ^{90,96}Zr, in comparison with CC calculations (see text). The ordinate is the second energy derivative of $E\sigma_{\rm fus}$ divided by πR_b^2, where the barrier position R_b is derived from the AW potential [31].

reproduces the separation between the two main peaks reasonably well, but it gives too much strength to the lower energy one. This calculation clearly underestimates the sub-barrier fusion cross sections (see previous section). The solid line is derived from the corresponding two-phonon calculation of Fig. 4. It gives a better overall fit to the experimental distribution, even if the distance between the two main peaks is too small.

The distribution of ^{48}Ca + ^{96}Zr has (at least) two peaks of comparable weight in the low-energy part, a hint of some structure around 96–97 MeV, and a high-energy bump at $\simeq$102 MeV. This shape with various well-defined peaks is quite different from the result for ^{40}Ca + ^{96}Zr studied previously [4]. The structure and overall shape of the present complex distribution are well reproduced only by the inclusion of three octupole phonons in ^{96}Zr, although the barrier around 93–94 MeV is calculated $\approx$1.5 MeV too high. The high-energy peak is well reproduced. The calculation with two phonons misses completely the shape of the distribution.

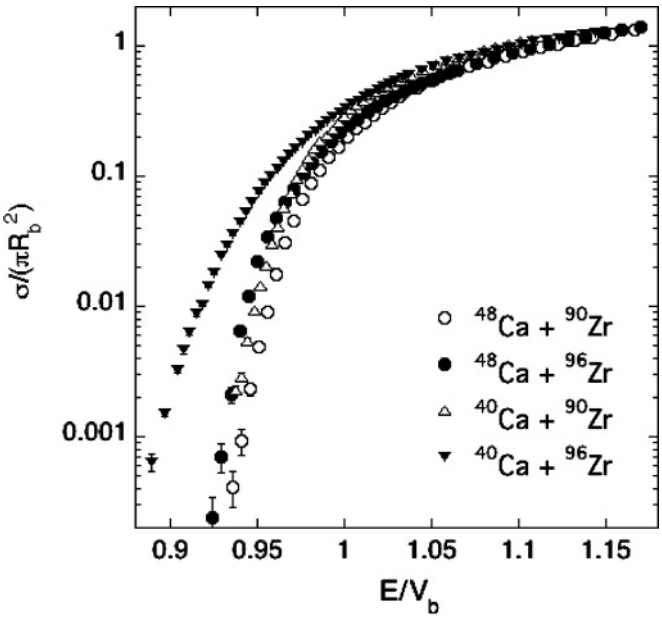

FIG. 7. Comparison of fusion cross sections of ^{40,48}Ca + ^{90,96}Zr.

VI. COMPARISON WITH ^{40}Ca + ^{90,96}Zr

Let us consider the present data for ^{48}Ca + ^{90,96}Zr and the older results [4] for the two systems involving ^{40}Ca as the beam and the same zirconium targets. We compare the excitation functions in the usual plot with reduced energy and cross sections scales, shown in Fig. 7 (see also Ref. [21]). The case of ^{40}Ca + ^{96}Zr clearly stands out from the others, both from the point of view of sub-barrier fusion enhancement and with respect to the slope of the excitation function in the same energy range, which is much flatter. The present observations do not agree with the predictions of Ref. [7].

There is no doubt that there is something special about that system. Identifying the reason(s) why this is so is an interesting challenge. Originally, one associated the experimental evidence with the availability, solely for ^{40}Ca + ^{96}Zr, of neutron-transfer channels with large and positive Q values [4]. Later, the dominant effect of the strong octupole vibration in ^{96}Zr was suggested [5]. However, we note that the excitation function for ^{48}Ca + ^{96}Zr (with no positive Q-values for transfer) is very similar to those for ^{40,48}Ca + ^{90}Zr. We also pointed out, in the previous section, that the three barrier distributions of ^{48}Ca + ^{96}Zr and ^{40,48}Ca + ^{90}Zr have a clear peak structure, at variance with the case of ^{40}Ca + ^{96}Zr. This leads us to conclude that the octupole vibration of ^{96}Zr is not the major factor in the dynamics. One may argue that, since ^{40}Ca (but not ^{48}Ca) has a well-known and strong octupole vibration, its combination (coupling) with the corresponding excitation of ^{96}Zr produces most of the effect, in a way that is not taken into account by the calculations of Ref. [4]. In any case, a strong influence of few- and multineutron transfer on fusion cannot be ruled out. The cumulative effect of several transfer channels, each giving a small contribution, might explain the evidence, especially at very low energies.

A step further in the comprehension of the dynamics might be achieved by measuring the intermediate case ^{40}Ca + ^{94}Zr,

where Q values for neutron transfer are still positive and large, but where the octupole vibration of ^{94}Zr is weaker and higher lying than in ^{96}Zr. In any case, one faces the continuing difficulty of performing full CC calculations where transfer couplings are explicitly taken into account.

VII. SUMMARY

Fusion-evaporation cross sections were measured in the two systems ^{48}Ca + ^{90,96}Zr in an energy range from well below to well above the Coulomb barrier. The analysis of the preliminary data [21] has been extended and completed. The excitation functions have been compared with the results of CC calculations [25]. One- and two-phonon octupole and quadrupole vibrations of ^{90,96}Zr were considered; it was necessary to consider even the three-phonon state of the strong and low-lying octupole vibration of ^{96}Zr to achieve good agreement with the data.

The low-energy slope of the excitation functions is directly related to the barrier width and hence to the diffuseness a of the WS potential used. For ^{48}Ca + ^{90}Zr, the AW value $a =$ 0.68 fm gives a good fit to the data, whereas a larger value $a = 0.85$ fm is needed for ^{48}Ca + ^{96}Zr. Indeed, the excitation function of ^{48}Ca + ^{96}Zr is steeper, as seen better in a plot of the logarithmic derivative of the cross section versus energy. Different values of $d\ \ln(E\sigma)/dE$ show up for the two systems at the lowest energies, although it is not entirely clear, for ^{48}Ca + ^{90}Zr, whether we have reached the expected low-energy plateau.

In the high-energy part of the excitation functions, the cross sections of ^{48}Ca + ^{96}Zr are very well fitted by calculations, which, however, overpredict the ^{48}Ca + ^{90}Zr data by 12%–13%. Such a discrepancy follows the trend discussed by Netwon *et al*. [9] for several systems where diffuseness parameters much larger than $a \approx 0.68$ fm were shown to be needed to reproduce above-barrier fusion cross sections. Here, a large diffuseness for ^{48}Ca + ^{90}Zr would bring the calculated cross sections very close to the data above the barrier, but the good fit at low energies would deteriorate. The underlying reason(s) must be clarified, as should the validity of the CC model based on a static nuclear potential with a WS shape [9]. Fusion data at deep sub-barrier energies [14] for ^{48}Ca + ^{90,96}Zr would be very interesting.

The barrier distribution for ^{48}Ca + ^{90}Zr, extracted from the data, is very similar to that of ^{40}Ca + ^{90}Zr. The distribution of ^{48}Ca + ^{96}Zr is wider, but it shows clear structures (peaks), at variance with the case of ^{40}Ca + ^{96}Zr. In a reduced plot of the excitation functions for these four systems, the sub-barrier data for ^{40}Ca + ^{96}Zr show a very large enhancement with respect to all other cases, which are bunched together. This evidence makes the phenomenological correlation to positive-Q-value transfer channels very plausible.

ACKNOWLEDGMENTS

We are very grateful to G. Pollarolo for fruitful discussions on various physical issues underlying this work. Grateful thanks are also due to the XTU Tandem staff for their professional work during the experiments and to Mr. M. Loriggiola and Mr. G. Manente for preparing targets of excellent quality.

[1] M. Dasgupta, D. J. Hinde, N. Rowley, and A. M. Stefanini, Annu. Rev. Nucl. Part. Sci. **48**, 401 (1998).
[2] A. B. Balantekin and N. Takigawa, Rev. Mod. Phys. **70**, 77 (1998).
[3] N. Rowley, G. R. Satchler, and P. H. Stelson, Phys. Lett. **B254**, 25 (1991).
[4] H. Timmers, L. Corradi, A. M. Stefanini, D. Ackermann, J. H. He, S. Beghini, G. Montagnoli, F. Scarlassara, G. F. Segato, and N. Rowley, Phys. Lett. **B399**, 35 (1997); H. Timmers, D. Ackermann, S. Beghini, L. Corradi, J. H. He, G. Montagnoli, F. Scarlassara, A. M. Stefanini, and N. Rowley, Nucl. Phys. **A633**, 421 (1998).
[5] G. Pollarolo and Å. Winther, Phys. Rev. C **62**, 054611 (2000).
[6] Å. Winther, Nucl. Phys. **A572**, 191 (1994); **A594**, 203 (1995); computer code GRAZING, http://www.to.infn.it/∼nanni/grazing.
[7] N. Wang, X. Wu, and Z. Li, Phys. Rev. C **67**, 024604 (2003).
[8] V. I. Zagrebaev, Phys. Rev. C **67**, 061601(R) (2003).
[9] J. O. Newton, R. D. Butt, M. Dasgupta, D. J. Hinde, I. I. Gontchar, C. R. Morton, and K. Hagino, Phys. Rev. C **70**, 024605 (2004); Phys. Lett. **B586**, 219 (2004).
[10] I. I. Gontchar, D. J. Hinde, M. Dasgupta, and J. O. Newton, Phys. Rev. C **69**, 024610 (2004).
[11] N. Rowley and A. C. Merchant, Astrophys. J. **381**, 591 (1991).
[12] C. Y. Wong, Phys. Rev. Lett. **31**, 766 (1973).
[13] C. L. Jiang, H. Esbensen, K. E. Rehm, B. B. Back, R.V. F. Janssens, J. A. Caggiano, P. Collon, J. Greene, A. M. Heinz, D. J. Henderson, I. Nishinaka, T. O. Pennington, and D. Seweryniak, Phys. Rev. Lett. **89**, 052701 (2002).
[14] C. L. Jiang, K. E. Rehm, H. Esbensen, R. V. F. Janssens, B. B. Back, C. N. Davids, J. P. Greene, D. J. Henderson, C. J. Lister, R. C. Pardo, T. Pennington, D. Peterson, D. Seweryniak, B. Shumard, S. Sinha, X. D. Tang, I. Tanihata, S. Zhu, P. Collon, S. Kurtz, and M. Paul, Phys. Rev. C **71**, 044613 (2005).
[15] C. L. Jiang, H. Esbensen, B. B. Back, R. V. F. Janssens, and K. E. Rehm, Phys. Rev. C **69**, 014604 (2004).
[16] K. Hagino, N. Rowley, and M. Dasgupta, Phys. Rev. C **67**, 054603 (2003).
[17] C. J. Lin, Phys. Rev. Lett. **91**, 229201 (2003).
[18] C. L. Jiang, H. Esbensen, K. E. Rehm, B. B. Back, R.V. F. Janssens, J. A. Caggiano, P. Collon, J. Greene, A. M. Heinz, D. J. Henderson, I. Nishinaka, T. O. Pennington, and D. Seweryniak, Phys. Rev. Lett. **91**, 229202 (2003).
[19] C. H. Dasso and G. Pollarolo, Phys. Rev. C **68**, 054604 (2003).
[20] B. G. Giraud, S. Karataglidis, K. Amos, and B. A. Robson, Phys. Rev. C **69**, 064613 (2004).
[21] F. Scarlassara, G. Montagnoli, S. Beghini, R. Silvestri, A. M. Stefanini, L. Corradi, B. R. Behera, E. Fioretto, S. Szilner, M. Trotta, Y. W. Wu, Z. H. Liu, M. Ruan, F. Yang, and H. Q. Zhang, Prog. Theor. Phys. Suppl. **154**, 31 (2004).
[22] A. M. Stefanini, D. Ackermann, L. Corradi, D. R. Napoli, C. Petrache, P. Spolaore, P. Bednarczyk, H. Q. Zhang, S. Beghini, G. Montagnoli, L. Mueller, F. Scarlassara, G. F. Segato, F. Soramel, and N. Rowley, Phys. Rev. Lett. **74**, 864 (1995).

[23] S. Beghini, C. Signorini, S. Lunardi, M. Morando, G. Fortuna, A. M. Stefanini, W. Meczynski, and R. Pengo, Nucl. Instrum. Methods A **239**, 585 (1985).
[24] A. M. Stefanini, M. Trotta, L. Corradi, A. M. Vinodkumar, F. Scarlassara, G. Montagnoli, and S. Beghini, Phys. Rev. C **65**, 034609 (2002).
[25] K. Hagino, N. Rowley, and A. T. Kruppa, Comput. Phys. Commun. **123**, 143 (1999).
[26] H. Esbensen, Phys. Rev. C **72**, 054607 (2005).
[27] A. T. Kruppa, P. Romain, M. A. Nagarajan, and N. Rowley, Nucl. Phys. **A560**, 845 (1993).
[28] K. Hagino, N. Takigawa, M. Dasgupta, D. J. Hinde, and J. R. Leigh, Phys. Rev. Lett. **79**, 2014 (1997).
[29] S. Raman, C. W. Nestor Jr., and P. Tikkanen, At. Data Nucl. Data Tables **78**, 1 (2001).
[30] T. Kibédi and R. H. Spear, At. Data Nucl. Data Tables **80**, 35 (2002).
[31] Ö. Akyüz and Å. Winther, in *Nuclear Structure and Heavy-Ion Physics, Proceedings of the International School of Physics "Enrico Fermi," Course LXXVII, Varenna*, edited by R. A. Broglia and R. A. Ricci (North Holland, Amsterdam, 1981).